CHEMICAL ENGINEERING TRANSACTIONS
VOL. 43, 2015
A publication of AIDIC
The Italian Association of Chemical Engineering
Online at www.aidic.it/cet
Chief Editors: Sauro Pierucci, Jiří J. Klemeš

ISBN 978-88-95608-34-1; **ISSN** 2283-9216
DOI: 10.3303/CET1543156

Water Gas Shift Reaction on Copper Catalysts Supported on Alumina and Carbon Nanofibers

Natália M. B. Oliveira*[a], Gustavo P. Valença[a], Ricardo Vieira[b]

[a]School of Chemical Engineering, State University of Campinas, Campinas (SP), Brazil
[b]Associated Laboratory of Combustion and Propulsion, National Institute for Space Research, Cachoeira Paulista (SP), Brazil
nataliaoliveira.eq@gmail.com

The water gas shift (WGS) reaction is widely used in the production of hydrogen, by the conversion of carbon monoxide into CO_2 and of water into H_2. In the present work, copper catalysts supported on alumina or carbon nanofibers (CNF) were used to study the WGS reaction. The catalysts were prepared by impregnating copper nitrate in the supports, with a nominal mass metallic content of 5%. The solids were dried, calcined and characterized by X-Ray Diffraction (XRD), nitrogen adsorption, nitrous oxide chemisorption and Inductively Coupled Plasma Optical Emission Spectrometry (ICP OES).
After calcination, the catalysts were loaded into the reactor, reduced and then tested in the WGS reaction at medium temperatures (398 – 573 K). The gases from reactor were analyzed online by Gas Chromatography (GC). The products were CO_2, H_2 and, probably, small amounts of coke. The CO partial pressure varied between 4.6 and 6.6 kPa, and the water partial pressure varied between 20.0 and 47.4 kPa.
Among the catalysts tested, 5% Cu/Al_2O_3 was the most active under all conditions used in this work, due to the high dispersion of the metal particles on the support. The most favorable reaction conditions for this catalyst were p^0_{H2O}*= 38.6 kPa* and p^0_{CO}*= 5.3 kPa* (H_2O:CO molar ratio of 7.3), for all reaction temperatures used in this work. Cu/CNF had low CO conversions, due to the support hydrophobicity. In case of this catalyst, the most favorable conditions were p^0_{H2O}*= 20.0 kPa* and p^0_{CO}*= 6.6 kPa*, corresponding to a H_2O:CO molar ratio of 3.1. The apparent activation energy calculated for the WGS reaction was 86.1 kJ mol^{-1} for 5% Cu/Al_2O_3 and 69.8 kJ mol^{-1} for 5% Cu/CNF. For Cu/CNF a co-operative redox reaction mechanism was proposed, and apparent reaction orders were 0.64 in relation to CO and approximately zero in relation to water.

1. Introduction

The water gas shift (WGS) reaction, $CO_{(g)} + H_2O_{(g)} \rightleftarrows CO_{2_{(g)}} + H_{2_{(g)}}$, is an important industrial reaction for the production of hydrogen. Hydrogen is used in fuel cells and in important processes, such as synthesis of ammonia and refining of fossil fuels by hydrocracking (Ratnasamy and Wagner, 2009; Palma et al., 2014). In addition, there is an increasing economic interest in the use of hydrogen as a transportable fuel, hydrogen being a promising substitute for gasoline and diesel (Chen et al., 2008).
Depending on the hydrogen application, the reactant gas compositions and the adopted reaction conditions may vary. According to Ratnasamy and Wagner (2009), the main problem is when the reaction products are present in reactor feed, since they are rate limiting.
The increasing economic interest in production of hydrogen makes the study of the WGS reaction highly attractive. The aim is to develop catalysts which are able to achieve conversions of carbon monoxide higher than those obtained on commercial catalysts such as $Cu/ZnO/Al_2O_3$ (Ratnasamy and Wagner, 2009). Although the reaction rate per unit volume is high on this catalyst, the stability under high temperature is low. In addition, industrial catalysts used in the WGS reaction have many weaknesses (Gunawardana et al., 2009). For example, the global system kinetics is very slow at temperatures at which chemical equilibrium is favorable, requiring a high mass of catalyst, that in turn results in long *in situ* reduction prior to reaction (Palma

Please cite this article as: Oliveira N., Valenca G., Vieira R., 2015, Water gas shift reaction on copper catalysts supported on alumina and carbon nanofibers, Chemical Engineering Transactions, 43, 931-936 DOI: 10.3303/CET1543156

et al., 2014). They are also sensitive to air, condensed water and sulfur. Thus, the demand for more robust catalysts, able to process different feedstocks, has led to the study of numerous solids as possible WGS catalysts (Grenoble et al., 1981; Li et al., 2000; Huber et al., 2007; Pazmiño et al., 2012).

Carbon nanofibers (CNF) can be an alternative catalytic support owing to its special structural features. They have prismatic planes on surface, which promote a better metal/support interaction. In addition, CNF have a high specific surface area, ideal for the formation of small metal particles. Carbon nanofibers also have high mechanical strength, because of the interweaving of fibers, and high electrical conductivity (Huber et al., 2007). However, according to Vieira et al. (2003), the nanometric size of the CNF (an average diameter of ca. 30 nm) can result in a large pressure drop in chemical reactors. In order to reduce pressure drop in packed beds, CNF in macroscopic form have been developed (Pham-Huu et al., 2001), which were used in this work.

In the present work we studied the WGS reaction on copper catalysts supported on CNF or alumina in the temperature range from 398 to 573 K. The reaction results were correlated to the physical and chemical properties of the catalysts.

2. Experimental

2.1 Catalysts preparation and characterization

The catalytic supports used in this work were γ-alumina (Harshaw Catalysts), with particle size between 1.00 and 1.41 mm, and carbon nanofibers in macroscopic form.

The carbon nanofibers used as catalytic support were prepared from a graphite felt (Seecil Carbon Technologies). First, the graphite felt was immersed in concentrated nitric acid (65% P.A.) for one hour to remove impurities and introduce oxygenated groups on its surface (Huber et al., 2007). Then, the felt was flushed out with distilled water and dried in an oven at 393 K for 12 hours. After, it was impregnated 2 wt% of nickel ($Ni(NO_3)_2.6H_2O$, 99%, Acrós Organics) on felt surface. Using a tubular quartz reactor, the material was submitted to a hot air flow to be calcined (623 K for 1 hour). After, it was reduced in H_2 at 673 K for 1 hour. The last step is the growth of carbon nanofibers on the felt surface. The reaction conditions are an ethane to H_2 volume ratio of 1:4 at 973 K for 2 hours. Finally, the CNF were cut in the format of cylindrical pellets.

It was impregnated 5 wt% of copper ($Cu(NO_3)_2.3H_2O$, 99%, Acrós Organics) on supports: CNF or γ-Al_2O_3. Next the solids were dried in an oven (12 hours at 393 K) and calcined under a continuous flow of synthetic air (3 hours at 573 K). After, it was the *in situ* reduction under H_2 flow (0.5 $cm^3\,s^{-1}$) for 2 hours at 623 K.

The catalysts were characterized by X-Ray Diffraction (XRD, Philips Analytical X'Pert PW3050), Inductively Coupled Plasma Optical Emission Spectrometry (ICP OES, PerkinElmer Elan DRC-e) and, for determining the specific surface area (S_{BET}) and pore volume, it was used nitrogen adsorption (BET method) in a Micromeritics ASAP 2020 surface analyzer.

The compounds are also characterized by chemisorption of nitrous oxide in a Micromeritics AutoChem II apparatus equipped with a thermal conductivity detector (TCD). The methodology used was an adaptation of the one described by Maciel et al. (2011). The experiment involved the following steps: oxidation of the sample (25 mg) with 0.50 $cm^3\,s^{-1}$ of O_2 at 573 K for 1 hour; reduction with 10% H_2/N_2 (0.83 $cm^3\,s^{-1}$), heating at 0.17 K s^{-1} from room temperature to 623 K; re-oxidation of the surface Cu^0 with N_2O (0.50 $cm^3\,s^{-1}$) at 333 K for 1 hour; finally, reduction with 10% H_2/N_2 (0.83 $cm^3\,s^{-1}$), heating at 0.17 K s^{-1} from room temperature to 623 K. Between the oxidation and reduction steps, N_2 passed through the samples for cooling. The amount of H_2 consumed in the second reduction was used to quantify copper dispersion (D_{Cu}), metallic surface area (S_{Cu}) and average copper particle size ($Ø_{Cu}$). Both Cu surface area and Cu particle size were calculated by assuming that the Cu/N_2O ratio was 2 and that the surface concentration of copper was $1.47x10^{19}$ atoms m^{-2}.

2.2 Catalytic tests

The catalytic tests were carried out in a 20 mm ID copper tubular reactor. The reactor was externally heated by an electric oven (Carbolite VST 12/300). A stainless steel fritted disk was placed halfway in the reactor to hold the catalyst. There was a saturator in reaction line responsible for feeding water vapor in the reactor. The stainless steel saturator (volume of 500 cm^3) was heated in a glycerin bath with a heater and magnetic stirrer (Velp Scientifica). The gaseous reaction mixture was sent to a gas chromatograph (PerkinElmer Clarus 500) with a thermal conductivity detector (TCD) and a Chromosorb 102 60/80 column 3.66 m in length and 1/8" OD. The liquid products were condensed at the reactor exit and analyzed in a Hewlett Packard HP 6890 chromatograph with a TCD and a Porapak Q 80/100 packed column 2 m in length and 1/8" OD.

The reaction temperature was varied between 398 and 573 K, with 25 K increments, for each reaction condition, namely, catalyst, p^0_{CO} and p^0_{H2O}. The pressure, measured by a manometer installed on reaction line, was kept at 121 kPa and the ambient temperature at 296 K. To evaluate the influence of reactants molar ratio, the saturator temperature ranged between 333 and 353 K, with intervals of 5 K, and CO and He flow rates were kept constant (0.0833 and 1.13 $cm^3\,s^{-1}$, respectively). Variations in the saturator temperature (T_{sat})

represented variations of water partial pressure in the range between 20.0 kPa and 47.4 kPa, according to the Antoine equation. The conversion (X_{CO}) was calculated as the ratio between total amount of CO consumed in the reaction (F^0_{CO} - F_{CO}) and molar flow of CO fed into the reactor (F^0_{CO}). The chemical reaction rate (r), assuming differential scheme of reaction was calculated according to Eq(1), where W is the mass of catalyst.

$$r\ (mol\ m_{Cu}^{-2}\ s^{-1}) = -r_{CO} = \frac{F^0_{CO}.X_{CO}}{W.S_{Cu}} \quad (1)$$

3. Results and discussion

3.1 Catalysts properties

The metal concentration of solids was determined by Inductively Coupled Plasma Optical Emission Spectrometry (ICP OES). The concentrations determined are 4.69% for Cu/CNF and 5.10% for Cu/Al_2O_3. The results show small relative errors between nominal (5 wt%) and real metal concentrations.

The data obtained from the samples reduction after N_2O chemisorption were used to calculate some solids properties. The copper dispersions (D_{Cu}) calculated are 65% for Cu/Al_2O_3 and 37% for Cu/CNF. The metal surface areas (S_{Cu}) are equal to 21.4 and 11.2 $m^2_{Cu}\ g^{-1}_{cat}$ for Cu/Al_2O_3 and Cu/CNF, respectively. And the average copper particle sizes ($Ø_{Cu}$) calculated are 1.6 for Cu/Al_2O_3 and 2.8 nm for Cu/CNF.

Supports and catalysts samples were analyzed by XRD technique and the crystalline phases were identified by comparing the diffraction patterns with those found at JCPDS (Joint Committee on Powder Diffraction Standards). The diffraction patterns of γ-Al_2O_3 and Cu/Al_2O_3 (Figure 1a) have six major peaks. The peaks at *2θ* equal to 37.1°, 45.9° and 67.0° correspond to reflections of γ-Al_2O_3 crystal planes (311), (400) and (440), respectively. The peaks at *2θ* equal to 14.5°, 28.2° and 49.2° refer to reflections of AlOOH crystal planes (020), (120) and (200), respectively. The peaks amplitude (a.u.) was low, which made diffraction patterns with noise and poorly defined peaks. No peaks for Cu diffraction were observed, suggesting that the metal was in amorphous state or highly dispersed on support. In addition, the crystallites were smaller ($Ø_{Cu}$ = 1.6 nm) than the lower detection limit of crystalline structures (4 nm) by XRD. The diffraction patterns for calcined CNF and Cu/CNF (Figure 1b) showed more defined spectral lines, with higher peak intensities, indicating the presence of large crystals. The first peak at *2θ = 26.4°* is characteristic of carbon crystallographic plane (002). The second peak at *2θ = 43.3°* can be assigned to the plane (012) of nickel oxide, present in both samples. This peak indicates a low dispersion of metal deposited to CNF formation, however it does not affect the felt covering, due to the nanofiber growth mechanism (Vieira et al., 2003). The peaks observed at *2θ = 35.7°* and 39.0° on the XRD patterns for Cu/CNF (Figure 1b) are characteristic of cupric oxide. These data are in agreement with the N_2O chemisorption results, i.e., the metal particles on CNF are larger and less dispersed than on alumina.

Nitrogen adsorption and desorption isotherms were measured at liquid N_2 temperature (77 K). The surface areas of the CNF and γ-Al_2O_3 samples, calculated according to the BET method, were 67.2 and 221 $m^2\,g^{-1}$, respectively. The carbon felt surface area, calculated by the BJH method, is small (<1 $m^2\,g^{-1}$), below the instrument detection limit, and consequently this result should be taken carefully. However, this result consists with Vieira et al. (2003) affirmation that the felt has an increase in specific area of approximately 100 times after the growth of CNF, in addition to the mass gain of 100%. The pore volume and diameter of the solids were also calculated by the BJH desorption method. The pore volumes were 0.2 $cm^3\,g^{-1}$ for CNF and 0.6 $cm^3\,g^{-1}$ for Al_2O_3. The pore diameters of 7.5 for Al_2O_3 and 11 nm for CNF are typical of mesoporous solids. However, it should be emphasized that nanofibers have a structure of interlaced filaments (Vieira et al., 2003).

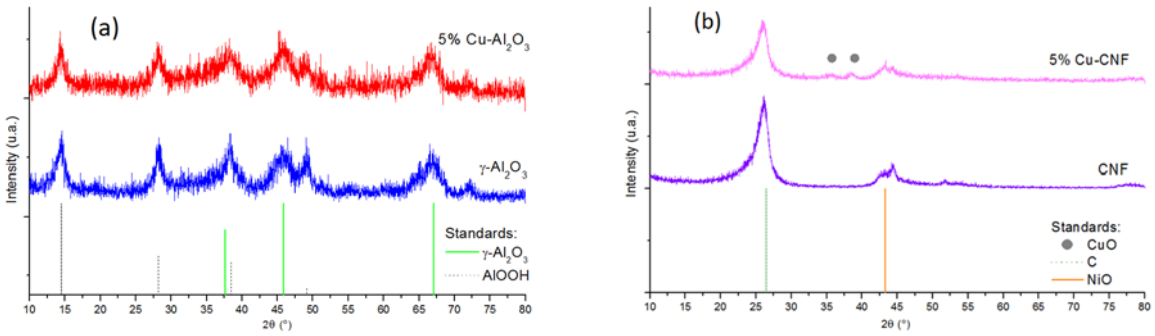

Figure 1: JCPDS standards and XRD patterns for calcined samples of γ-Al_2O_3 and 5% Cu/Al_2O_3 (a) and CNF and 5% Cu/CNF (b).

The values of textural properties obtained for calcined alumina were close to those provided by manufacturer: S_{BET} = 234 $m^2 g^{-1}$, pore volume 0.65 $cm^3 g^{-1}$ and pore diameter smaller than 30 nm. The larger alumina surface area favors the dispersion of active agents. However, the low specific area of the CNF does not necessarily imply lower efficiency or catalytic performance unsatisfactory, due to its peculiar structure in fiber, which tends to favor products diffusion and reactants accessibility to catalyst active sites.

3.2 Catalysts activities

Blank tests were carried out without catalyst, to make sure that under the reaction conditions used in this work, the WGS reaction did not occur on the copper reactor wall. In addition, blank tests also carried out with only CNF. In both cases no product was observed suggesting that the nickel particles used to grow the CNF remained completely covered with a thin carbon layer as suggested Huber et al. (2007).

The water partial pressure was varied by changing the saturation temperature (T_{sat}) and keeping the CO volumetric flow rate constant and equal to 0.083 $cm^3 g^{-1}$, then different molar ratios of reactants were achieved (H_2O:CO from 3.1 to 10). An increase in p^0_{H2O} up to 38.6 kPa resulted in an increase in amount of CO consumed for copper catalysts supported on γ-alumina (Figure 2a). However, when p^0_{H2O} increased from 38.6 to 47.4 kPa a decrease in CO conversion was observed, indicating that the excess amount of water caused a saturation of the catalyst. Similar results were already obtained. Chen et al. (2008) found that CO conversion increases if steam to CO ratio increases. However, according to these authors, the performance of WGS reaction is insensitive to variations in ratio if H_2O:CO is greater than 4. Excessive steam feeding the WGS reaction has two beneficial effects: increases equilibrium conversion (Chen et al., 2008) and disfavors coke formation (Ratnasamy and Wagner, 2009). It is concluded therefore that for Cu/Al_2O_3, reaction conditions most appropriate is water partial pressure equal to 38.6 kPa when volumetric flow rate of CO is 0.083 $cm^3 g^{-1}$, that is a H_2O:CO molar ratio of 7.3.

For copper catalysts supported on CNF (Figure 2b) the CO conversion was lower than in the case of Cu/Al_2O_3 and varied between 0 and 12%. These results are in agreement with the S_{Cu} values which show the metal surface area of Cu/Al_2O_3 higher than that of Cu/CNF. Moreover, since CNF are hydrophobic, the WGS reaction maybe was impaired on this support as the adsorption of water is necessary for the reaction to proceed. An increase in p^0_{H2O} resulted in a decrease in the conversion of CO, except when p^0_{H2O} changed from 31.3 to 38.6 kPa (Figure 2b). The highest X_{CO} occurred for the lowest p^0_{H2O} applied and reactants molar ratio (H_2O:CO) of 3.1.

Comparing the catalysts Cu/Al_2O_3 and Cu/CNF, alumina proved to be a catalyst support more appropriate than CNF for application in the WGS reaction. There is a correlation between the profiles of CO conversion obtained and the results from XRD and N_2O chemisorption. Signs referring to copper were not observed for 5% Cu/Al_2O_3 (Figure 1a), whereas characteristic peaks of CuO were detected for 5% Cu/CNF (Figure 1b). These were confirmed by N_2O chemisorption results, copper particles on alumina were smaller and more dispersed than on CNF, i.e., there was a greater amount of exposed metal, which explains the better catalytic performance of 5% Cu/Al_2O_3. According to Gunawardana et al. (2009), high catalytic activity of copper supported on alumina in the WGS reaction is explained by the force of interaction between adsorbate (CO) and adsorbent (Cu/Al_2O_3), showing that interaction between them is optimal, that is, it is strong enough.

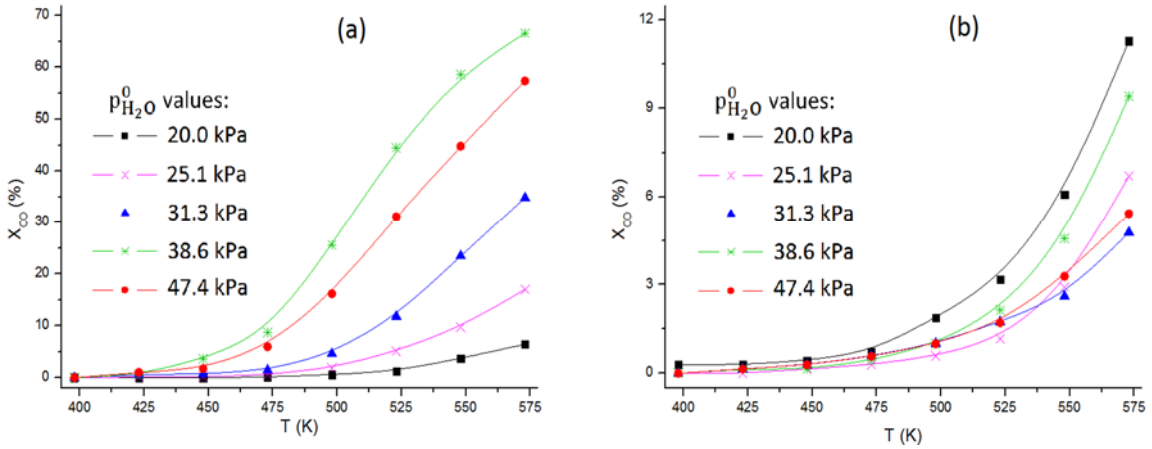

Figure 2: CO conversion at WGS reaction on 5% Cu/Al_2O_3 (a) and 5% Cu/CNF (b) catalysts as a function of reaction temperature for various p^0_{H2O}, with $q^0_{CO} = 0.083\ cm^3 s^{-1}$.

3.3 Kinetics measurements

Among the possible stoichiometric reactions, only WGS reaction and coke formation ($CO + H_2 \rightarrow C + H_2O$) occurred. No methanol or formaldehyde was observed under the experimental conditions used in this work. The possibility of methane formation was also eliminated by analyzing gaseous products.

The molar flow of CO and CO_2 were obtained by gas chromatography and used to calculate the carbon balance. It was assumed that the difference in carbon balance corresponds to coke produced. Since the errors obtained were mostly between 0 and 1%, with a maximum value of 5.62%, the coke formation was small. The catalytic activity was expressed by CO disappearance rate ($-r_{CO}$), which was divided into two parts: $-r_{CO(1)}$ consumed in the WGS reaction (Eq1) and $-r_{CO(2)}$ consumed in the secondary reaction (coke formation).

The catalytic reaction velocity can be expressed empirically (Eq2), considering for this the influence of composition (Power Law) and temperature (Arrhenius equation). A is the pre-exponential factor, E_a is the activation energy (kJ mol^{-1}), R is the gas constant (kJ mol^{-1} K^{-1}), T is the absolute temperature (K), C_i is the component i concentration and α_i is the reaction order in relation to component i.

$$r = A.\exp\left(-\frac{E_a}{R.T}\right).C_i^{\alpha_i} \quad (2)$$

However, Eq(2) does not consider the physical-chemical nature of the reaction and can be used only in the conditions in which data was fitted. Thus, a rate equation based on the reaction mechanism was evaluated. Li et al. (2000) studied the WGS reaction on Cu- and Ni-loaded cerium oxide catalysts and proposed the Eq(3) for the reaction rate. They based on a co-operative redox reaction mechanism, involving two irreversible steps at stead state: ($H_2O + * \rightarrow H_2 + O*$) and ($O* + CO_{(a)} \rightarrow CO_2 + *$).

$$r = \frac{A_1.A_2.exp\left[-\frac{Ea_1+Ea_2}{R.T}\right].p_{CO}.p_{H_2O}}{A_1.exp\left[-\frac{Ea_1}{R.T}\right].p_{CO}+A_2.exp\left[-\frac{Ea_2}{R.T}\right].p_{H_2O}} \quad (3)$$

The fittings of the reaction data ($-r_{CO(1)}$, calculated by Eq1) to the rate equations (Eq2 and Eq3) were used to determine equations parameters and to evaluated if the mechanism proposed by Li et al. (2000) explains our experimental data satisfactorily. It was not obtained good fit of reaction data on 5% Cu/Al_2O_3 to Eq(3), indicating that the sequence of elementary steps proposed by Li et al. (2000) does not represent the activity of this catalyst in the WGS reaction. Power Law (Eq2) fits reasonably to experimental data ($R^2 = 0.84$). However, the reaction orders obtained were very high, 4.1 for CO and 5.9 for H_2O, which probably are incorrect, since normally the orders sum varies between -3 and 3. In this case, the activation energy of reaction was determined to be 86.1 kJ mol^{-1}. The lack of fit of data for 5% Cu/Al_2O_3 may have been caused by the lower amount of experimental points (36 points) concentrated in a narrow temperature range (398 – 473 K).

The fittings of reaction data for the catalyst 5% Cu/CNF were good for both equations. The largest amount of experimental data (55 points) in a wider range of reaction temperatures (398 – 573 K) gives reliability to the fits. The determination coefficient (R^2) was 0.90 for Eq(3), allowing to affirm that the mechanism of the WGS reaction on Cu/CNF is co-operative redox-type, as already reported Li et al. (2000). By fitting the data to Power Law (Eq2), it was possible to determine the apparent orders of reaction, being 0.64 for CO and approximately zero for H_2O, and the apparent activation energy equals to 69.8 kJ mol^{-1}.

The study of Grenoble et al. (1981) presents an apparent activation energy of 55.7 ± 3.3 kJ mol^{-1} for 10% Cu/Al_2O_3, evaluated in a temperature range of 323 a 573 K. This result differs significantly from the obtained in this work for 5% Cu/Al_2O_3 (86.1 kJ mol^{-1}). It should be noted that in this study a small temperature range was evaluated and the metal content was just half of that. In addition, those authors studied the support influence for platinum catalysts and showed that Pt supported on Al_2O_3 and SiO_2 have almost the same apparent activation energy (82.0 ± 5.4 kJ mol^{-1} and 79.9 ± 3.3 kJ mol^{-1}, respectively). However, when the catalyst is Pt/C there is a significant increase in E_a, approximately 30%. This result also differs from the obtained in the present work for copper-based catalysts. It was observed here that changing support, from alumina to CNF, represents a decrease of almost 20% in the apparent activation energy.

Similar results to those observed for the catalyst 5% Cu/CNF had been obtained by Campbell and Daube (1987) when they investigated the WGS reaction rates on surface of a Cu (111) crystal. It has therefore that the catalyst studied here behaved similarly to pure metal. That is, support exerted little influence on the catalytic performance of the solid, since there are no interactions between metal and CNF. This is also in agreement with results obtained by XRD and N_2O chemisorption, as the cupric oxide crystallites identified in 5% Cu/CNF (Figure 1b) confirm the presence of large metal particles. This conclusion is confirmed by low conversions obtained (Figure 2b), since large metal particles represent less metal exposure and low catalyst activity, causing that catalyst behaves like pure metal.

4. Conclusions

The molar ratio of reactants (H_2O:CO) was evaluated by varying the partial pressure of water. It was observed that high values of p^0_{H2O} tended to favor the WGS reaction for the catalyst Cu/Al_2O_3. Meanwhile, for the Cu/CNF catalyst, it was observed no tendency between the variations of X_{CO} and p^0_{H2O}. Cu/CNF showed the highest activity when p^0_{H2O} was the lowest value evaluated and H_2O:CO was 3.1.

It was admitted that there was coke formation in very small amounts, considering the molar balance of compounds present in the reaction. The reaction data were fitted to the rate equations proposed (Eq2 and Eq3) to suggest a possible sequence of elementary steps for the reaction and to determine some reaction parameters. The mechanism proposed by Li et al. (2000) represents satisfactorily the experimental data of Cu/CNF, suggesting that the reaction mechanism is a co-operative redox-type for this catalyst. For 5% Cu/CNF catalyst, in the reaction conditions studied, the apparent activation energy is 69.8 kJ mol^{-1} and the apparent reaction orders for CO and H_2O are 0.64 and -0.02, respectively. Similar results had been obtained for Cu (111) (Campbell and Daube, 1987), suggesting that the support almost does not influence the catalytic performance of Cu/CNF. This fact agrees with the large copper particles identified by XRD, causing that the solid behaved similarly to pure metal. Large particles also represent less metal exposure and low catalytic activity. In addition, catalysts Cu/CNF had low activity due to the support hydrophobicity, which hinders water adsorption and, thus, the WGS reaction. Among the catalysts tested, 5% Cu/Al_2O_3 showed the best results in the WGS reaction. The high dispersion of Cu on alumina accounted for great exposure of metal on catalytic surface and consequently for a high activity.

References

Campbell C.T., Daube K.A., 1987, A surface science investigation of the water-gas shift reaction on Cu(111), Journal of Catalysis, 104, 109-119, DOI: 10.1016/0021-9517(87)90341-1.

Chen W-H., Hsieh T-C., Jiang T.L., 2008, An experimental study on carbon monoxide conversion and hydrogen generation from water gas shift reaction, Energy Conversion and Management, 49, 2801-2808, DOI: 10.1016/j.enconman.2008.03.020.

Grenoble D.C., Estadt M.M., Ollis D.F., 1981, The chemistry and catalysis of the water gas shift reaction: 1. The kinetics over supported metal catalysts, Journal of Catalysis, 67, 90-102, DOI: 10.1016/0021-9517(81)90263-3.

Gunawardana P.V.D.S., Lee H.C., Kim D.H., 2009, Performance of copper-ceria catalysts for water gas shift reaction in medium temperature range, International Journal of Hydrogen Energy, 34, 1336-1341, DOI: 10.1016/j.ijhydene.2008.11.041.

Huber F., Yu Z., Walmsley J.C., Chen D., Venvik H.J., Holmen A., 2007, Nanocrystalline Cu-Ce-Zr mixed oxide catalysts for water-gas shift: carbon nanofibers as dispersing agent for the mixed oxide particles, Applied Catalysis B: Environmental, 71, 7-15, DOI: 10.1016/j.apcatb.2006.08.013.

Li Y., Fu Q., Flytzani-Stephanopoulos M., 2000, Low-temperature water-gas shift reaction over Cu- and Ni-loaded cerium oxide catalysts, Applied Catalysis B: Environmental, 27, 179-191, DOI: 10.1016/S0926-3373(00)00147-8.

Maciel C.G., Profeti L.P.R., Assaf E.M., Assaf J.M., 2011, Hydrogen purification for fuel cell using CuO/CeO_2-Al_2O_3 catalyst, Journal of Power Sources, 196, 747-753, DOI: 10.1016/j.jpowsour.2010.07.061.

Palma V., Pisano D., Martino M., Ricca A., Ciambelli P., 2014, Comparative studies of low temperature water gas shift reaction over platinum based catalysts, Chemical Engineering Transactions, 39, 31-36, DOI: 19.3303/CET1439006.

Pazmiño J.H., Shekhar M., Williams W.D., Akatay M.C., Miller J.T., Delgass W.N., Ribeiro F.H., 2012, Mettalic Pt as active sites for the water-gas shift reaction on alkali-promoted supported catalysis, Journal of Catalysis, 286, 279-286, DOI: 10.1016/j.jcat.2011.11.017.

Pham-Huu C., Vieira R., Charbonnière L., Ziessel R., Ledoux M.J., 2001, Composites à base de nanotubes ou nanofibres de carbone déposés sur un support active pour application en catalyse, French Patent 0115178, assigné à SiCat.

Ratnasamy C., Wagner J.P., 2009, Water gas shift catalysis, Catalysis Reviews, 51:3, 325-440, DOI: 10.1080/01614940903048661.

Vieira R., Pham-Huu C., Keller N., Ledoux M.J., 2003, Novos materiais à base de nanofibras de carbono como suporte de catalisador na decomposição da hidrazina, Química Nova, 26:5, 665-669, DOI: 10.1590/S0100-40422003000500008.